EEG Acquisition in Ultra-High Static Magnetic Fields up to 9.4T.

Article *in* NeuroImage · December 2012

DOI: 10.1016/j.neuroimage.2012.11.064 · Source: PubMed

8 authors, including:

Irene Neuner
Forschungszentrum Jülich
67 PUBLICATIONS **932** CITATIONS
SEE PROFILE

Tracy Warbrick
Brain Products GmbH
50 PUBLICATIONS **777** CITATIONS
SEE PROFILE

Martina Reske
Forschungszentrum Jülich
57 PUBLICATIONS **1,308** CITATIONS
SEE PROFILE

Frank Boers
Forschungszentrum Jülich
61 PUBLICATIONS **697** CITATIONS
SEE PROFILE

NeuroImage 68 (2013) 214–220

Contents lists available at SciVerse ScienceDirect

NeuroImage

journal homepage: www.elsevier.com/locate/ynimg

EEG acquisition in ultra-high static magnetic fields up to 9.4 T

Irene Neuner [a,b,d,*,1], Tracy Warbrick [a,1], Jorge Arrubla [a], Jörg Felder [a], Avdo Celik [a], Martina Reske [a], Franks Boers [a], N. Jon Shah [a,c,d]

[a] Institute of Neuroscience and Medicine 4, INM 4, Forschungszentrum Jülich, Germany
[b] Department of Psychiatry, Psychotherapy and Psychosomatics, RWTH Aachen University, Germany
[c] Department of Neurology, RWTH Aachen University, Germany
[d] JARA-BRAIN — Translational Medicine, Germany

ARTICLE INFO

Article history:
Accepted 30 November 2012
Available online 14 December 2012

Keywords:
Ultra high field
MR
EEG
Cardiac-related artefact

ABSTRACT

The simultaneous acquisition of electroencephalographic (EEG) and functional magnetic resonance imaging (fMRI) data has gained momentum in recent years due to the synergistic effects of the two modalities with regard to temporal and spatial resolution. Currently, only EEG-data recorded in fields of up to 7 T have been reported. We investigated the feasibility of recording EEG inside a 9.4 T static magnetic field, specifically to determine whether meaningful EEG information could be recovered from the data after removal of the cardiac-related artefact. EEG-data were recorded reliably and reproducibly at 9.4 T and the cardiac-related artefact increased in amplitude with increasing B0, as expected. Furthermore, we were able to correct for the cardiac-related artefact and identify auditory event related responses at 9.4 T in 75% of subjects using independent component analysis (ICA). Also by means of ICA we detected event related spectral perturbations (ERSP) in subjects at 9.4 T in response to opening/closing the eyes comparable with the response at 0 T. Overall our results suggest that it is possible to record meaningful EEG data at ultra-high magnetic fields. The simultaneous EEG-fMRI approach at ultra-high-fields opens up the horizon for investigating brain dynamics at a superb spatial resolution and a temporal resolution in the millisecond domain.

Introduction

Simultaneous multimodal brain imaging is motivated by the synergistic effect of combining the high temporal resolution of electrophysiological measurements with the high spatial resolution of functional magnetic resonance imaging (fMRI) (Blinowska et al., 2009; De Martino et al., 2010; Debener and De Vos, 2011; Debener and Herrmann, 2008; Debener et al., 2006; Logothetis, 2008, 2012; Makeig et al., 2004; Neuner et al., 2010; Ostwald et al., 2010). As such, the simultaneous acquisition of electrophysiological and fMRI data has gained momentum in recent years. Recording these multiple measures of brain activity at the same time, under the same physiological and psychological conditions is advantageous for many aspects of cognitive neuroscience, in particular, pharmacological challenge studies, sleep studies, studies investigating epilepsy or evoked potential studies such as the P300 with regard to age (Debener et al., 2008; Juckel et al., 2012; Koike et al., 2011).

As fMRI at ultra high fields opens the road to higher spatial resolution aiming at a columnar (Yacoub et al., 2008) and laminar level its relationship to EEG signals recorded at the scalp level remains a concern. The electrical signal measured with scalp electrodes represents synchronised activity from widespread cortical regions. This would seem at odds with the increased spatial resolution achieved in the fMRI data at ultra-high magnetic fields. However, the strength of the EEG data lies in the temporal resolution which is complementary to the relatively slow haemodynamic response. Using the EEG we are able to model rapidly changing brain dynamics in the order of milliseconds to guide the analysis of the fMRI data. For example, epileptic spikes can be identified in the EEG data providing highly accurate 'events' for analysing the high resolution fMRI data, the different stages of sleep can be identified guiding analysis of sleep states, or cognitive ERP components, such as the P300, can be used to determine when a decision regarding a stimulus has been made. The progression to higher field strengths does not impact on the temporal resolution of the EEG so it is still valuable for the same reasons as at lower field strengths. As fMRI signals will be acquired at ultra high fields from increasingly localised volumes the degree to which EEG and fMRI data will agree (i.e. a problem of understanding macroscopic neurovascular coupling) needs detailed investigation.

However, simultaneous acquisition comes at a price; artefacts from gradient switching as well as cardiac-related artefacts contaminate the EEG signal (Mullinger et al., 2008). The artefact resulting from gradient switching is relatively easy to correct for due to fact that it is generated by the MR scanner and therefore consistently reproducible across a recording session (Allen et al., 2000). The cardiac-related artefact on the other hand is far more variable, both across subjects and within the

* Corresponding author at: Institute for Neuroscience and Medicine 4, INM4, Forschungszentrum Jülich, 52428 Jülich, Germany. Fax: +49 2461 611919.
E-mail address: i.neuner@fz-juelich.de (I. Neuner).
[1] These authors contributed equally.

1053-8119/$ – see front matter © 2012 Elsevier Inc. All rights reserved.
http://dx.doi.org/10.1016/j.neuroimage.2012.11.064

same individual across a recording session. The precise source of cardiac-related artefact is unclear but it is related to a number of factors including pulsatile blood movement, small head movements and scalp expansion. The ballistic effect is thought to be due to motion induced in the subject's body as blood is pumped upwards. Movement of electrically conductive material in a magnetic field results in electromagnetic induction; as such, the motion related to cardiac activity can lead to electromotive forces in the circuit between the subject and the recording equipment, thus resulting in artefact in the recording. In addition to this ballistic effect there is also a cardiac-related artefact due to the Hall effect where a small voltage is induced by the abrupt changes in blood flow velocity in proximity to the electrodes (Debener et al., 2008). Furthermore, the size of the cardiac-related artefact is proportional to static field strength (Debener et al., 2008), making progression to recording electrophysiological signals at ultra high fields problematic.

Limited information is available regarding the feasibility of simultaneous electrophysiological recording in ultra high magnetic fields with reports in the literature being available up to 7 T (Debener et al., 2008) while MR scanners of higher field strength are becoming available. Debener et al. (2008) compared the behaviour of the cardiac-related artefact at three different field strengths (1.5, 3 T, 7 T). Based on theoretical assumptions (Tenforde et al., 1983) of the Lorentz' law, they showed the amplitude of the cardiac-related artefact to be directly proportional to the strength of the magnetic field. However, they tested the amplifier capabilities, artefact correction procedures and resulting data quality up to 7 T. In order to transfer the advantages of simultaneous EEG-fMRI described above to ultra high field investigation of the nature of the cardiac-related artefact at field strengths higher than 7 T is necessary. It is unclear at what field strength the critical threshold lies for a) technical aspects: amplifier, cap recording capability and b) size and degree of distortion of the cardiac-related artefact being too large for correction.

To this end we aimed to investigate the feasibility of recording usable electrophysiological data at ultra high fields by answering the following questions:

a) How does the cardiac-related artefact change across different static magnetic field strengths: 0 T (earth field), 4 T, 7 T, 8 T and 9.4 T?
b) Can ERPs be retrieved from data recorded in ultra high magnetic fields?
c) Can meaningful information regarding the spectral quality of the EEG be retrieved from data recorded in ultra high magnetic fields?

Methods

We present 3 studies addressing the questions stated above in turn. All studies were conducted independently with different samples.

Subjects

For study 1 (see below for details on each study) EEG data were recorded in 5 healthy volunteers (2 female) with a mean age of 25.4 (SD 1.8) years. For study 2 EEG data were recorded from 16 healthy subjects (3 female) with a mean age of 30 (SD 10.8) years. For study 3, 8 healthy male volunteers were recruited aged 30 (SD 4.5) years. Written informed consent was obtained from all subjects and the study was approved by the local ethics committee.

Procedures

Study 1: nature of the cardiac-related artefact at ultra-high fields

EEG data were recorded from each subject outside of the scanner (0 T) and at four different field strengths inside a Siemens 9.4 T human whole body scanner (Siemens Medical Systems, Erlangen, Germany). Measurements outside the scanner were performed with the subject in a supine position to be consistent with scanner environment. Inside the scanner the patient table was positioned in a field of 4 T (1850 mm from the isocentre), 7 T (1450 mm from the isocentre), 8 T (1300 mm from the isocentre) and 9.4 T (isocentre). Subjects were moved slowly to the required position in the scanner and a 5 minute adaptation period was allowed before recording. Following the adaptation period a 6 minute resting state (eyes closed) recording was performed at each field strength. One subject stopped the experiment after 8 T due to claustrophobia moving further towards the isocentre.

Study 2: auditory ERPs

EEG responses to auditory stimuli were recorded at 0 T and 9.4 T. The 0 T measurements were performed in a mock scanner where the scanner environment can be realistically created without the effects of the static field on the EEG signal. For the 9.4 T recordings the scanner described above was used and subjects were positioned at the isocentre of the scanner. After an adaptation period of 5 minute auditory stimuli were delivered via headphones using Presentation software (Version: 11.0, Neurobehavioral Systems. Albany, California) and an external driver unit for earspeakers (model SRM-252II. STAX Ltd. Saitama, Japan). Extension cables made of copper and crystal wire were set between the driver unit and the headphones (model SRE-750. STAX Ltd. Saitama, Japan). The stimulation consisted of 200 tones at a frequency of 1000 Hz, duration of 500 ms and a sound pressure of 88 dB. There was a delay of 26 ms between the stimuli marker in the EEG recording and the actual presenting of the tones to the volunteers. The sequence of stimuli was randomised and the inter-stimulus interval had a variance between 2000 and 14000 ms.

Study 3: detecting changes in alpha power

EEG data were recorded from each subject outside of the scanner (0 T) and 9.4 T (isocentre) inside the scanner. Measurements outside the scanner were performed with the subject in a supine position to be consistent with scanner environment. For the measurements inside the scanner subjects were moved slowly to the required position and a 5 minute adaptation period was allowed before recording. Following the adaptation period EEG data was recorded for 6 min while the subject alternated between an eyes open and an eyes closed state. Each eyes open and eyes closed period was 30 s in length resulting in 6 blocks of each condition. Subjects were prompted to open/close their eyes with a verbal cue given via the scanner intercom. When the command to open or close the eyes was given verbally over the intercom system a marker (1 for open the eyes, 2 for close the eyes) was set manually in the EEG recorder software.

EEG data acquisition

For all studies EEG data were recorded using Brain Vision Recorder (Brain Products, Gilching, Germany) and a 32-channel MR compatible EEG system (Brain Products, Gilching, Germany). The EEG cap (BrainCap MR, EasyCap GmbH, Breitbrunn, Germany) consisted of 29 scalp electrodes distributed according to the 10-20 system and three additional electrodes, one of which was attached to the subjects' back for recording the electrocardiogram (ECG), while the others were attached on the outer canthus of each eye for detection of ocular artefacts. Data were recorded relative to a Cz reference and a ground electrode was located at Iz (10-5 electrode system, Oostenveld and Praamstra, 2001). Data were sampled at 5000 Hz, with a bandpass of 0.016–250 Hz. Impedance at all recording electrodes was less than 10 kΩ. During data acquisition the helium pump of the 9.4 T pilot system was kept running.

EEG data analysis

Study 1: nature of the cardiac-related artefact at ultra-high fields

To correct for cardiac-related artefact the R peaks of the ECG wave were detected using the semi-automatic peak detection method in BrainVision Analyzer 2 (Brain Products, Gilching, Germany). Raw EEG data were then corrected for cardiac-related artefact using an Optimal

Basis Set (OBS) method (Niazy et al., 2005, Centre for Functional MRI of the Brain (FMRIB), Oxford University, UK), which is available as a plug-in to EEGLAB (http://sccn.ucsd.edu/eeglab/, Delorme and Makeig, 2004). The OBS method developed by Niazy et al. (2005) involves identifying basis functions describing temporal variation in the artefact using temporal principal components analysis (PCA). These basis functions were then fitted to and subtracted from the EEG. For further details of this method see Niazy et al. (2005). After correction for cardiac-related artefact data were down-sampled to 250 Hz and exported to BrainVision Analyzer 2 (Brain Products, Gilching, Germany) for further processing.

To compare the amplitude of the cardiac-related artefact across the different field strengths the data were segmented based on the R peak of the ECG-wave (−500–1500 ms, with the R peak positioned at zero), averaged and baseline corrected. To make sure that the number of events included in the average did not differ across subjects or field strengths, and thus impact the SNR, the first 300 heartbeat events were taken for each subject. The largest distortions in the ECG as a result of the magnetic field appear to be in the T wave (see Fig. 1B). This can also be observed in the artefact in the EEG channels (Fig. 2). To quantify the change in this wave across field strengths, the peak amplitude in a window 150 ms–550 ms post R peak was measured from the ECG channel and two EEG channels T7 and T8.

Study 2: auditory ERPs

Data recorded at 9.4 T were corrected for cardiac-related artefact using the procedure described for Study 1. Using EEGLAB the corrected 9.4 T data and data recorded at 0 T (mock scanner) were down-sampled to a rate of 250 Hz, re-referenced to an average reference and filtered at 0.16–20 Hz with a notch filter 45–55 Hz. Data were then segmented around the event markers, 50 ms before the event and 250 after, resulting in segments of 300 ms. Segment rejection was performed by visual inspection in search of muscle and high amplitude artefacts. The presence of auditory evoked potentials was first evaluated at channel level in temporal channels (TP9, TP10). The presence of ERPs was also evaluated at independent component (IC) level as described below. The non-excluded segments were subjected to extended infomax ICA (Lee et al., 1999) using the runica algorithm (Makeig et al., 1997) including all of the EEG channels and excluding all of the non-EEG. This was achieved using the toolbox included in EEGLAB. The resulting independent components were then inspected for topography, ERP signal, and consistency across single trials to determine event related potential components. The topographic criterion for choosing suspect components carrying the ERP signal was a distribution of positive signals arising in the temporal lobes. The shape of the signal was then evaluated in the temporal channels (TP9 and TP10), where clear positive signal with a latency between 90 and 140 ms was sought (P100). In this regard, the data recorded at 0 T in channel level data served as example for latency and shape when choosing the components. The choosing/rejection

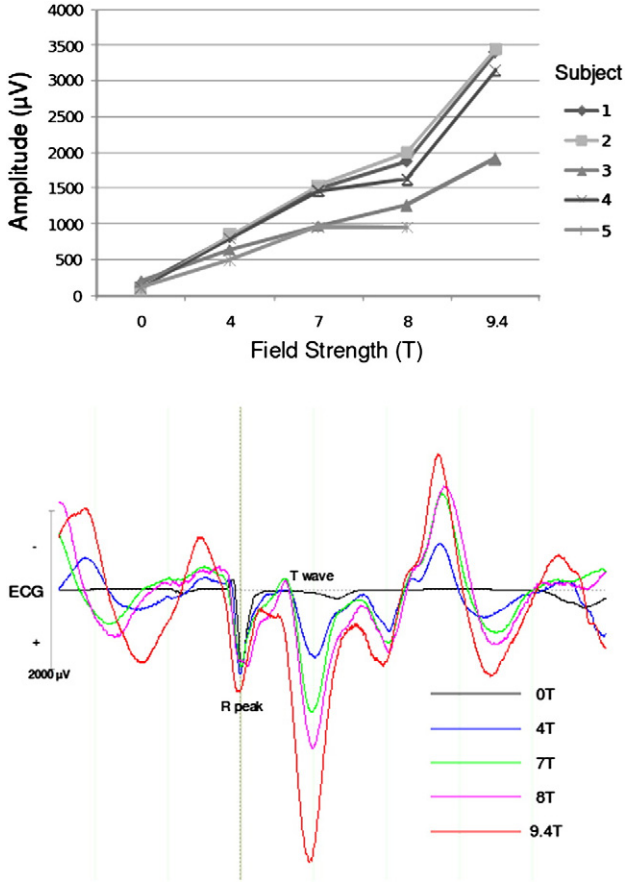

Fig. 1. A. Maximum amplitude of the T wave of the ECG signal in all subjects at all field strengths (data from 9.4 T missing for subject number 5). B. The ECG wave across all field strengths for one representative subject (Subject 3). The same pattern of increasing amplitude with increasing field strength can be seen for the other subjects in Supplementary Fig. 1.

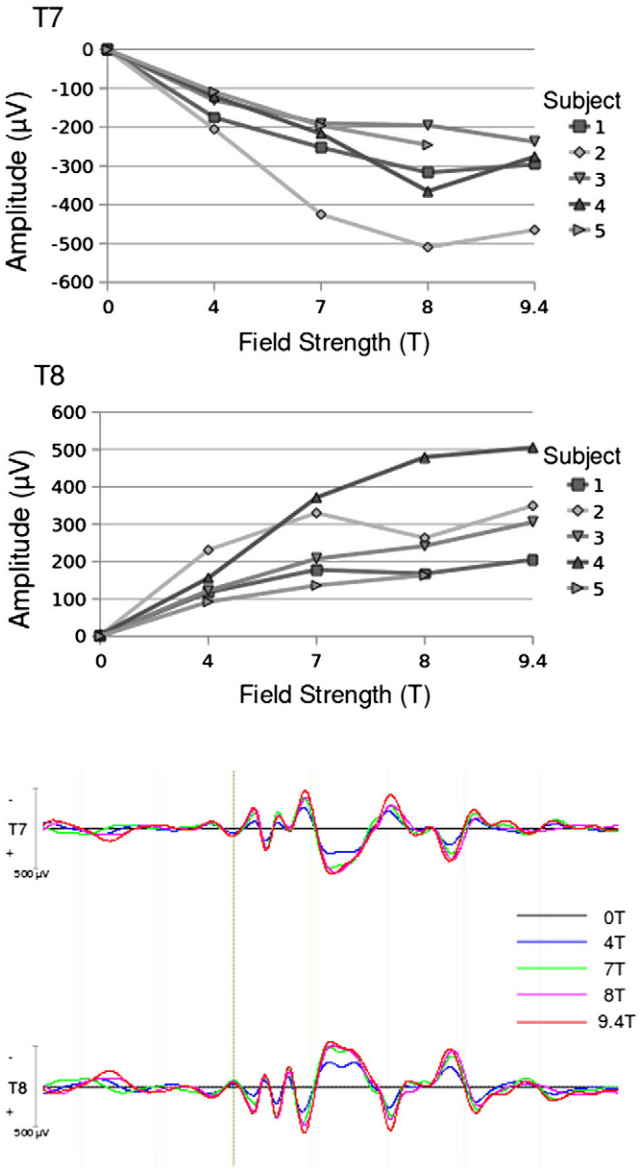

Fig. 2. A. Maximum amplitude of the cardiac-related artefact in the T7 and T8 EEG channels in all subjects at all field strengths (data from 9.4 T missing for subject number 5). B. The cardiac-related artefact in the T7 and T8 electrodes across all field strengths for one representative subject.

of ICA components was always performed by the same operator. The chosen components were kept while the rest were excluded. Amplitude and latency values of the resulting signals at TP9 were exported for statistical analysis.

Study 3: detecting changes in alpha power

For reduction of the cardiac-related artefact OBS was performed as described above in study 1. A different correction method involving ICA was also attempted for data recorded at 9.4 T as described below. The data were first analysed in Brain Vision Analyzer (Version 2.02, Brain Products, Gilching, Germany), down-sampled to a rate of 250 Hz, re-referenced to average and corrected for cardiac-related artefact using ICA (Vanderperren et al., 2010). In order to obtain independent components (IC) a restricted Infomax ICA algorithm was applied to the whole data, including 512 steps and automatic determining of the components with eigenvalue trigger of 0.001. The cardiac-related artefact correction was accomplished by visual identification of components contributing the artefact and rejecting them using the 'Inverse ICA' tool. The choosing/rejection of ICA components was always performed by the same operator. The resulting datasets of both correction methods, OBS and ICA, were analysed further in EEGLAB. No filtering was applied.

The segmentation was achieved with respect to the 'Open eyes' event, 4 s before the event and 4 s after. A first evaluation was performed at channels O1 and O2 using the ERSP (event related spectral perturbation) time-frequency plot function in EEGLAB to determine whether alpha desynchronisation could be observed upon opening the eyes. This was performed for data recorded at 0 T and at 9.4 T after correction with OBS and ICA. The presence of alpha desynchronisation was evaluated at IC level as described below. The segmented data were also subjected to restricted infomax ICA (Lee et al., 1999) using runica (Makeig et al., 1997) from the EEGLAB toolbox. The resulting independent components were inspected to determine whether a component representing alpha power could be found; the topography, trial-to-trial frequency changes and a peak in the power spectrum between 8 and 12 Hz were used as criteria for determining components representing the alpha rhythm of the EEG. Those components fulfilling the criteria were kept while the rest were excluded. The ERSP (event related spectral perturbation) time–frequency plot function in EEGLAB was used to determine whether alpha desynchronisation could be observed upon opening the eyes. This was performed on the O1 and O2 channels.

Results

Study 1: nature of the cardiac-related artefact at ultra high fields

The degree of distortion in the ECG wave and the amplitude of the cardiac-related artefact increases with field strength. The maximum amplitude of the T wave of the ECG signal for all subjects at all field strengths can be seen in Fig. 1, illustrating the increase in amplitude with increasing field strength. An example of the distortion in the waveform from one representative subject is displayed in the lower part of Fig. 1. It also demonstrates the increasing extent of distortion with increasing field strength. In addition to the distortion of the ECG signal itself the cardiac-related artefact in the EEG channels was also influenced by the field strength. The maximum amplitude of the cardiac-related artefact in the EEG channels T7 and T8 in all subjects at all field strengths can be seen in Fig. 2, along with an example of the EEG data from one representative subject.

The distortion of the ECG wave showed a trend for an exponential increase in amplitude, this can be seen on the left hand side of Supplementary Fig. 1, while the cardiac-related artefact in the EEG channels showed a trend for a linear increase in amplitude with increasing field strength (Supplementary Fig. 1). These effects were reproducible across subjects.

Furthermore, we were able to correct for the cardiac-related artefact at all field strengths. Supplementary Fig. 2 shows the uncorrected and corrected data for one representative subject on the segmented data at temporal electrodes (left hand side of figure) and in continuous data for a number of electrodes across field strengths, illustrating the correction of the artefact.

Study 2: auditory ERPs

Clear ERPs in 15 out of 16 subjects were identified at channel level data at 0 T but only traces of ERPs were found in 3 subjects at 9.4 T static magnetic fields (Supplementary Fig. 3). Independent components representing clear bilateral auditory ERPs were found in all 16 subjects at 0 T. However in the 9.4 T scanner data from only 12 subjects yielded clear auditory ERPs, in 10 cases bilaterally and in 2 cases just on one side (Supplementary Fig. 4). Data from two representative subjects can be seen in Fig. 3. Paired *t*-test showed no significant difference in the latencies of the auditory P100 recorded at 0 T ($M = 130.25$, $SD = 9.46$) and at 9.4 T ($M = 130.50$, $SD = 16.32$) static magnetic fields; $t(15) = -0.63$, $p = 0.951$. There was a significant difference in the amplitude of auditory P100 recorded at 0 T ($M = 3.98$, $SD = 2.04$) and at 9.4 T ($M = 10.42$, $SD = 6.05$) static magnetic fields; $t(15) = -4.806$, $p < 0.001$. Topographic views of the signal average across the 16 subjects under both conditions can be seen in Fig. 4.

Study 3: detecting changes in alpha power

Clear alpha desynchronisation upon opening the eyes was observed in 7 subjects at the channel level at 0 T (Supplementary Fig. 5). The data recorded at 9.4 T static field and corrected using OBS did not show the same effect neither at channel level nor at IC level (Supplementary Fig. 6). The data recorded at 9.4 T and corrected using ICA showed some degree of alpha desynchronisation at channel level only in 2 cases (Supplementary Fig. 5). All eight subjects in the 0 T field at the independent components level showed alpha desynchronisation. The same effects could be observed in 6 out of 8 subjects at 9.4 T when the data were corrected for cardiac-related artefact using the ICA approach (Supplementary Fig. 7). The results at 0 T and 9.4 T (using ICA for cardiac-related artefact) from one representative subject can be seen in Fig. 5.

Discussion

We investigated the feasibility of recording EEG inside a 9.4 T static magnetic field, specifically to determine whether meaningful EEG information could be recovered from the data after removal of the cardiac-related artefact. With our ERP paradigm we were able to identify auditory event related responses at 9.4 T in 75% of subjects using ICA. We were able to detect event related spectral changes in 75% of subjects at 9.4 T applying ICA. From a feasibility perspective the EEG amplifier continued to record steadily throughout the session. The volunteers did not report any difference in perception of the EEG-cap at the different field strengths. One volunteer reported a metallic taste when speaking in the magnet at 9.4 T, a known potential side effect at 9.4 T independent of the EEG-set up. Overall our results suggest that it is possible to record meaningful EEG data at ultra high magnetic fields, however, the nature of the required response and the design of the stimulation paradigm need to be carefully considered. We discuss our findings below.

In line with the limited data available up to fields of 7 T the cardiac-related artefact appears to increase linearly with field strength, whereas the ECG waveform itself shows a trend for an exponential increase in amplitude. The cardiac-related artefact waveform continues to vary substantially between individuals. In addition to the inter- and intra-individual variability in the artefact the known spatial variability e.g. between occipital and temporal electrodes is preserved at ultra-high fields. Despite increases in the amplitude of the cardiac-related artefact up to 9.4 T it is possible to remove it from the EEG in order to allow further assessment of the EEG signal.

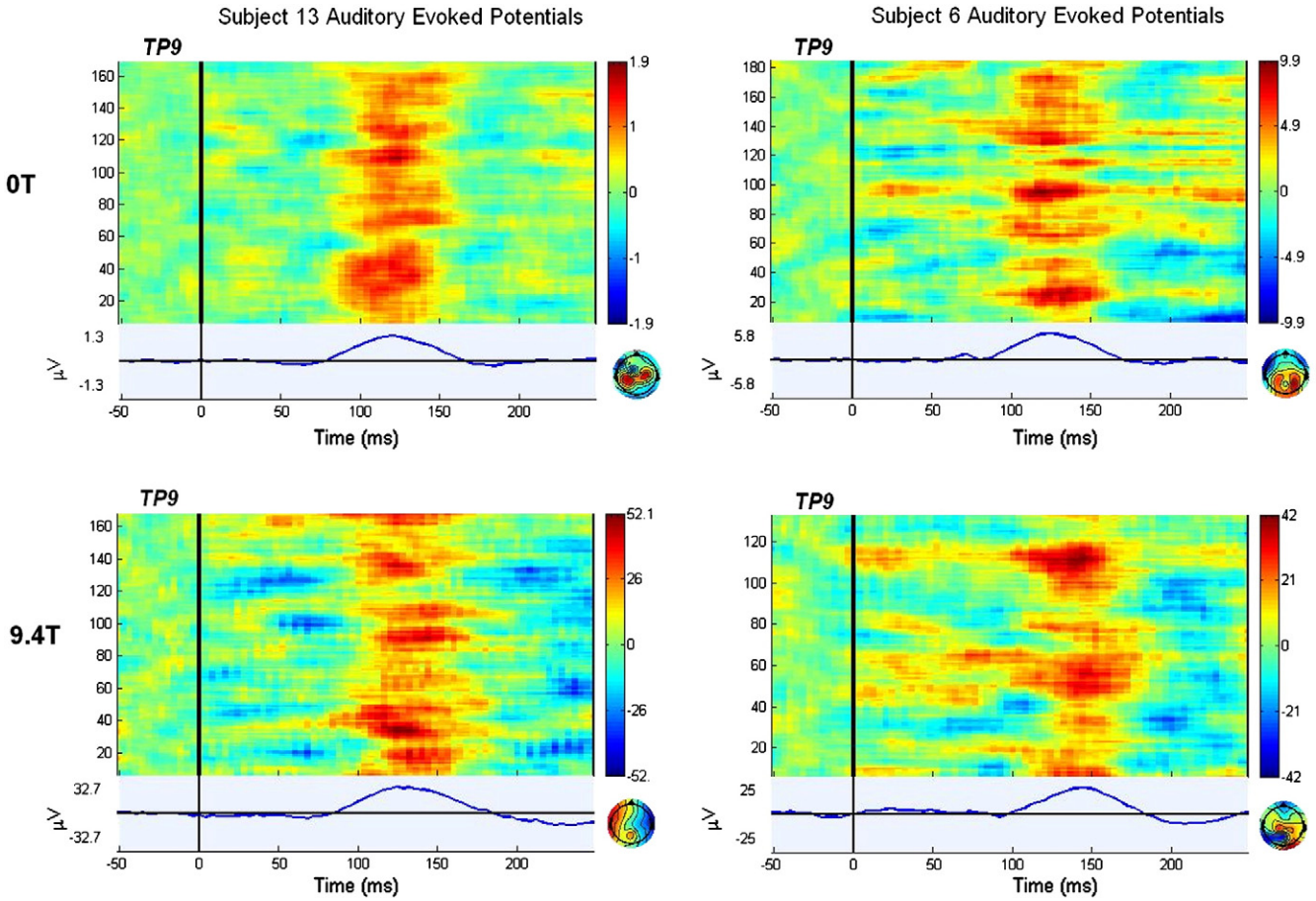

Fig. 3. Examples of auditory evoked potentials at 0 T and 9.4 T for two representative subjects and projected to channel TP9.

We were able to retrieve ERPs from data recorded in the 9.4 T field, however this was only possible when using ICA to identify relevant brain responses, when the 9.4 T data were analysed at channel level it was not possible to identify auditory evoked potentials in all cases (Supplementary Fig. 3). We propose that this is due to residual artefact in the data after correction for cardiac-related artefact. ICA provides a way to separate signal from noise components, thus allowing us to observe event related responses. On the other hand, the paired *t*-test revealed no significant difference of the ERP latencies at IC level in EEG recorded at 0 T compared with 9.4 T. However, the amplitudes of the

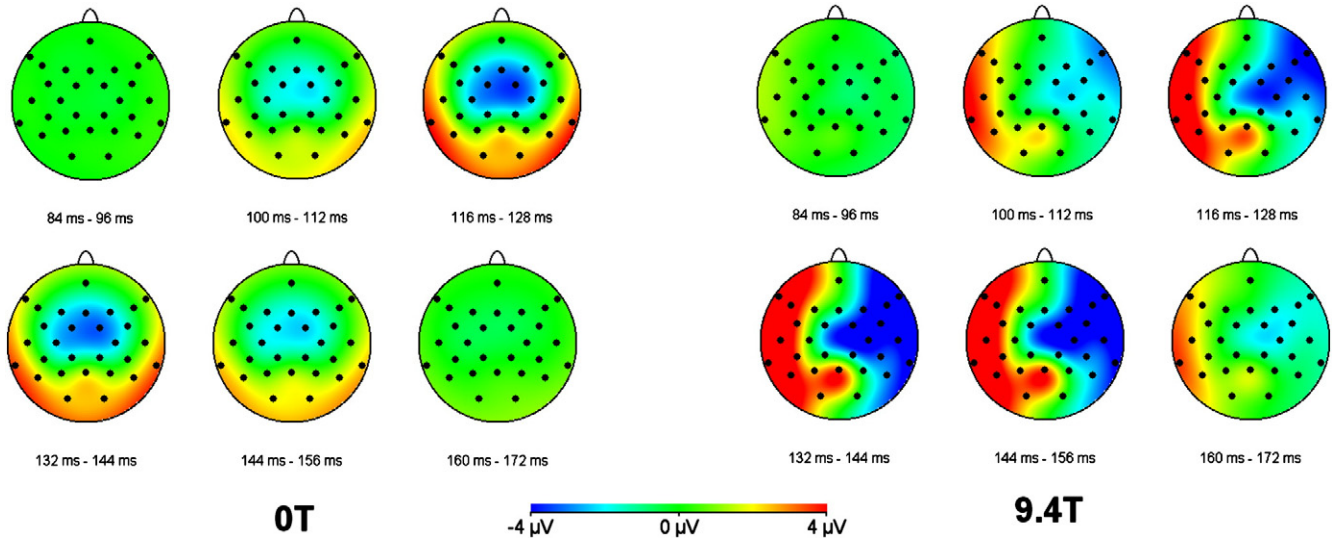

Fig. 4. Topographic view of the signal average corresponding to left auditory ERPs in 16 subjects in data recorded at 0 T and 9.4 T after correction of cardiac-related artefact and independent component analysis. The topographies of the ERPs varied to quite a degree between both field strengths. We propose that this is due to remaining artefacts in the 9.4 T signals.

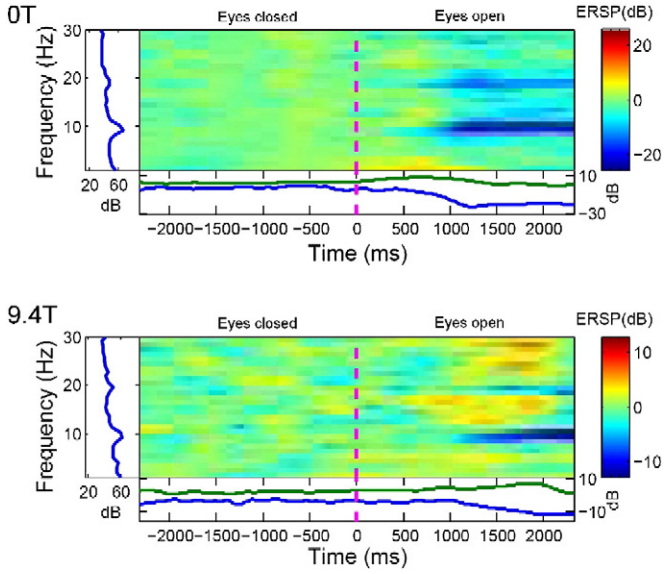

Fig. 5. Example of ERSP time-frequency analysis in one representative subject at 0 T and 9.4 T projected to channel O1. The desynchronisation of the frequencies between 8 and 10 Hz (alpha desynchronisation) can be observed. The data recorded at 9.4 T were corrected for cardiac-related artefact using ICA.

ERPs at 0 T compared to 9.4 T differed being higher at 9.4 T. Amplitudes might be affected by the parameters of auditory stimulation and by the applied correction methods in order to remove the cardiac-related artefact from the 9.4 T data. Since we kept the stimulation parameters constant with the help of stimulation through in-ear devices we discuss the differences in amplitude as a result of potential sub-optimal correction of the data from the cardiac-related artefact. In our first correction approach, using the cardiac-related artefact correction method described by Allen and colleagues (Allen et al., 1998), the correction led to a complete subtraction of the evoked signal. With the OBS approach the cardiac-related artefact was not completely removed and the recording at such a high magnetic field induces a large degree of distortion in the evoked potential signal. The topographies of the ERPs also varied to quite a degree between both field strengths (Fig. 4). We propose that this is due to remaining artefacts in the 9.4 T signals. Further research into optimising the processing of raw signals recorded at 9.4 T is necessary. These aspects need further investigation and further developments on optimization of correction steps.

We were also able to detect event related spectral perturbations (ERSP) in the 9.4 T field comparable to the 0 T field in the alpha frequency in 75% of subjects upon opening and closing the eyes. Again, our results were present at 9.4 T when using ICA but not at the channel level. As described above, we attribute the absence of ERSPs and auditory evoked potentials at channel level at 9.4 T to residual noise in the data after artefact correction. It must be mentioned that OBS was sufficient for correction of the cardiac-related artefact to yield auditory ERPs at IC level, but not for finding ERSP. Thus, we needed to explore ICA for cardiac-related artefact correction in order to find alpha-desynchronisation.

Recording electrophysiological data in ultra high fields up to 9.4 T holds great promise but also numerous challenges. From a technical point of view our data show that electrophysiological recordings in an ultra high magnetic field of 9.4 T are possible. From an electrophysiology point of view one can conclude that evoked potentials and ERSPs can be recorded at ultra high magnetic fields. In epilepsy research simultaneous fMRI-EEG recordings have become an important diagnostic tool in pre-neurosurgery assessment and in treatment resistant cases (Kim et al., 2011). Based on epilepsy specific EEG graphoelements such as spikes, spike-waves or sharp waves an EEG informed fMRI analysis can be performed to help identify the epileptoform focus or network. In a case where MRI at clinical field strengths does not reveal a structural lesion the ultra-high MR imaging, also with the benefits of new contrasts, could help to improve structural assessment. The simultaneously acquired EEG would answer the question whether a detected lesion is also likely to be functionally relevant in the genesis of epileptic activity (Thornton et al., 2011).

The combination of fMRI and EEG is an essential tool in the classification of sleep stages. The focus of recent sleep research has been the functional connectivity between subcortical and cortical areas and the change of connectivity pattern during different sleep stages (Duyn, 2012; Sämann et al., 2011). The elucidation of factors or connectivity patterns that contribute to the effectiveness of sleep, the mechanisms forming the basis for memory consolidation and differentiation of healthy sleep from abnormal sleep in psychiatric and neurological disorders are also pertinent topics in current sleep research. Concurrent EEG sets the stage for sleep pattern analysis and allows for an investigation on a functional/spatial level of certain sleep phenomena such as K-complexes.

Functional imaging has a longstanding task-related focus in MRI and EEG can provide information on task related brain events on a millisecond timescale. Since the description of ongoing “resting state” activity by Biswal and colleagues, the concept of the resting state and the so-called default network has become a popular field of fMRI research (Biswal et al., 1995; Damoiseaux and Greicius, 2009; Fox and Greicius, 2010). During resting-state experiments the classic instruction of a subject would be “to close the eyes, think of nothing specific and do not fall asleep”. Given this unspecific instruction a parameter for the vigilance state of the subject during the resting state fMRI data acquisition is desirable. EEG recordings offer this information, being the basis for sleep staging according to Rechtschaffen and Kales stadia as a gold standard. A recent talk by Helmut Laufs at the third biennial conference of resting state brain connectivity in Magdeburg, Germany (07.09.2012) showed that during resting state paradigms the potential confound introduced by falling asleep with altered functional connectivities could be substantial (Laufs, 2012). As monkey experiments indicate a laminar functional connectivity pattern, the high resolution images obtained at ultra high fields could help to achieve this in humans in vivo with EEG contributing from two main perspectives. One would be for monitoring the vigilance state of the subject during recording. Our results indicate that this is likely to be feasible. Secondly, a simultaneous EEG-fMRI approach at ultra-high-fields opens up the horizon for a detailed assessment of laminar specific functional connectivity at a precise temporal resolution in the millisecond domain. Furthermore it would allow one to investigate brain dynamics in deeper detail. The presence of ERSPs due to eyes opening/closing opens the horizon for spectral analysis. Spontaneous dynamic oscillations could be analysed with regard to their origin and spreading pattern (Logothetis, 2012; Makeig et al., 2004).

A further challenge will arise with the addition of gradient artefacts for fMRI investigations. These data need to be replicated within an fMRI experiment, to determine the effects of gradient artefact removal on data quality at ultra high fields. In MRI the magnetic field gradients determine parameters such as spatial resolution, field-of-view, and slice-thickness. The strengths of the applied gradients for a chosen imaging parameter set are independent of field strength and the artefacts arising from gradient switching are deterministic in nature. Further, since the superposition of the gradient fields on top of the static magnetic field can be treated using vectors, it is readily anticipated that artefacts arising from gradient switching will be removable at ultra high field using standard strategies borrowed from lower fields.

Conclusions

Our pilot study in healthy volunteers demonstrates the feasibility of electrophysiological recordings in static magnetic fields up to 9.4 T. The cardiac-related artefact increases linearly in field strength and the need for correction is substantial due to the large amplitude and

high degree of distortion of the artefact. For averaged electrophysiological signals such as auditory evoked potentials a correction of the cardiac-related artefact applying OBS is successful on ICA level basis, but not on channel level. For the analysis of event related spectral pertubations in the alpha range only a combination of ICA for correction of the cardiac-related artefact as well as for signal analysis proved to be successful. Further lines of research will focus on objectives measures for the ICA based signal analysis.

Supplementary data to this article can be found online at http://dx.doi.org/10.1016/j.neuroimage.2012.11.064.

Acknowledgements

We kindly acknowledge funding by the BMBF (Grant number 13N9121) and Siemens for the 9.4 T project. We thank Ingmar Gutberlet and Robert Stürmer for stimulating discussions.

References

Allen, P.J., Polizzi, G., Krakow, K., Fish, D.R., Lemieux, L., 1998. Identification of EEG events in the MR scanner: the problem of pulse artefact and a method for its subtraction. NeuroImage 8, 229–239.
Allen, P.J., Josephs, O., Turner, R., 2000. A method for removing imaging artefact from continuous EEG recorded during functional MRI. NeuroImage 12, 230–239.
Biswal, B., Yetkin, F.Z., Haughton, V.M., Hyde, J.S., 1995. Functional connectivity in the motor cortex of resting human brain using echo-planar MRI. Magn. Reson. Med. 34, 537–541.
Blinowska, K., Muller-Putz, G., Kaiser, V., Astolfi, L., Vanderperren, K., Van Huffel, S., Lemieux, L., 2009. Multimodal imaging of human brain activity: rational, biophysical aspects and modes of integration. Comput. Intell. Neurosci. 813607.
Damoiseaux, J.S., Greicius, M.D., 2009. Greater than the sum of its parts: a review of studies combining structural connectivity and resting-state functional connectivity. Brain Struct. Funct. 213, 525–533.
De Martino, F., Valente, G., de Borst, A.W., Esposito, F., Roebroeck, A., Goebel, R., Formisano, E., 2010. Multimodal imaging: an evaluation of univariate and multivariate methods for simultaneous EEG/fMRI. Magn. Reson. Imaging 28, 1104–1112.
Debener, S., De Vos, M., 2011. The benefits of simultaneous EEG-fMRI for EEG analysis. Clin. Neurophysiol. 122, 217–218.
Debener, S., Herrmann, C.S., 2008. Integration of EEG and fMRI. Editorial. Int. J. Psychophysiol. 67, 159–160.
Debener, S., Ullsperger, M., Siegel, M., Engel, A.K., 2006. Single-trial EEG-fMRI reveals the dynamics of cognitive function. Trends Cogn. Sci. 10, 558–563.
Debener, S., Mullinger, K.J., Niazy, R.K., Bowtell, R.W., 2008. Properties of the ballistocardiogram artefact as revealed by EEG recordings at 1.5, 3 and 7 T static magnetic field strength. Int. J. Psychophysiol. 67, 189–199.
Delorme, A., Makeig, S., 2004. EEGLAB: an open source toolbox for analysis of single-trial EEG dynamics including independent component analysis. J. Neurosci. Methods 134, 9–21.
Duyn, J.H., 2012. EEG-fMRI methods for the study of brain networks during sleep. Front. Neurol. 3, 100.
Fox, M.D., Greicius, M., 2010. Clinical applications of resting state functional connectivity. Front. Syst. Neurosci. 4, 19.
Juckel, G., Karch, S., Kawohl, W., Kirsch, V., Jäger, L., Leicht, G., Lutz, J., Stammel, A., Pogarell, O., Ertl, M., Reiser, M., Hegerl, U., Möller, H.J., Mulert, C., 2012. Age effects on the P300 potential and the corresponding fMRI BOLD-signal. NeuroImage 60, 2027–2034.
Kim, Y.H., Kang, H.C., Kim, D.S., Kim, S.H., Shim, K.W., Kim, H.D., Lee, J.S., 2011. Neuroimaging in identifying focal cortical dysplasia and prognostic factors in pediatric and adolescent epilepsy surgery. Epilepsia 52, 722–727.
Koike, T., Kan, S., Misaki, M., Miyauchi, S., 2011. Connectivity pattern changes in default-mode network with deep non-REM and REM sleep. Neurosci. Res. 69, 322–330.
Laufs, H., 2012. Resting state experiments are heavily confounded by vigilance fluctuations. 3rd Biennial Conference on Resting Sate Brain Connectivity, 5–7 September. Magdeburg, Germany.
Lee, T.W., Girolami, M., Sejnowski, T.J., 1999. Independent component analysis using an extended infomax algorithm for mixed sub-Gaussian and super-Gaussian sources. Neural Comput. 11, 609–633.
Logothetis, N.K., 2008. What we can do and what we cannot do with fMRI. Nature 453, 869–878.
Logothetis, N.K., 2012. Intracortical recordings and fMRI: an attempt to study operational modules and networks simultaneously. NeuroImage 62, 962–969.
Makeig, S., Jung, T.P., Bell, A.J., Ghahremani, D., Sejnowski, T.J., 1997. Blind separation of auditory event-related brain responses into independent components. Proc. Natl. Acad. Sci. U. S. A. 94, 10979–10984.
Makeig, S., Debener, S., Onton, J., Delorme, A., 2004. Mining event-related brain dynamics. Trends Cogn. Sci. 8, 204–210.
Mullinger, K., Brookes, M., Stevenson, C., Morgan, P., Bowtell, R., 2008. Exploring the feasibility of simultaneous electroencephalography/functional magnetic resonance imaging at 7 T. Magn. Reson. Imaging 26, 968–977.
Neuner, I., Stöcker, T., Kellermann, T., Ermer, V., Wegener, H.P., Eickhoff, S.B., Schneider, F., Shah, N.J., 2010. Electrophysiology meets fMRI: neural correlates of the startle reflex assessed by simultaneous EMG-fMRI data acquisition. Hum. Brain. Mapp. 31, 1675–1685.
Niazy, R.K., Beckmann, C.F., Iannetti, G.D., Brady, J.M., Smith, S.M., 2005. Removal of FMRI environment artefacts from EEG data using optimal basis sets. NeuroImage 28, 720–737.
Oostenveld, R., Praamstra, P., 2001. The five percent electrode system for high-resolution EEG and ERP measurements. Clin. Neurophysiol. 112, 713–719.
Ostwald, D., Porcaro, C., Bagshaw, A.P., 2010. An information theoretic approach to EEG-fMRI integration of visually evoked responses. NeuroImage 49, 498–516.
Sämann, P.G., Wehrle, R., Hoehn, D., Spoormaker, V.I., Peters, H., Tully, C., Holsboer, F., Czisch, M., 2011. Development of the brain's default mode network from wakefulness to slow wave sleep. Cereb. Cortex 21, 2082–2093.
Tenforde, T.S., Gaffey, C.T., Moyer, B.R., Budinger, T.F., 1983. Cardiovascular alterations in Macaca monkeys exposed to stationary magnetic fields: experimental observations and theoretical analysis. Bioelectromagnetics 4, 1–9.
Thornton, R., Vulliemoz, S., Rodionov, R., Carmichael, D.W., Chaudhary, U.J., Diehl, B., Laufs, H., Vollmar, C., McEvoy, A.W., Walker, M.C., Bartolomei, F., Guye, M., Chauvel, P., Duncan, J.S., Lemieux, L., 2011. Epileptic networks in focal cortical dysplasia revealed using electroencephalography-functional magnetic resonance imaging. Ann. Neurol. 70, 822–837.
Vanderperren, K., De Vos, M., Ramautar, J.R., Novitskiy, N., Mennes, M., Assecondi, S., Vanrumste, B., Stiers, P., Van den Bergh, B.R., Wagemans, J., Lagae, L., Sunaert, S., Van Huffel, S., 2010. Removal of BCG artefacts from EEG recordings inside the MR scanner: a comparison of methodological and validation-related aspects. NeuroImage 50, 920–934.
Yacoub, E., Harel, N., Ugurbil, K., 2008. High-field fMRI unveils orientation columns in humans. Proc. Natl. Acad. Sci. U. S. A. 105, 10607–10612.